Accepted Manuscript

Design, synthesis and bioevaluation of antitubulin agents carrying diaryl-5,5-fused-heterocycle scaffold

Qile Xu, Maolin Sun, Zhaoshi Bai, Yueting Wang, Yue Wu, Haiqiu Tian, Daiying Zuo, Qi Guan, Kai Bao, Yingliang Wu, Weige Zhang

PII: S0223-5234(17)30436-1

DOI: 10.1016/j.ejmech.2017.05.065

Reference: EJMECH 9495

To appear in: *European Journal of Medicinal Chemistry*

Received Date: 5 April 2017

Revised Date: 16 May 2017

Accepted Date: 31 May 2017

Please cite this article as: Q. Xu, M. Sun, Z. Bai, Y. Wang, Y. Wu, H. Tian, D. Zuo, Q. Guan, K. Bao, Y. Wu, W. Zhang, Design, synthesis and bioevaluation of antitubulin agents carrying diaryl-5,5-fused-heterocycle scaffold, *European Journal of Medicinal Chemistry* (2017), doi: 10.1016/j.ejmech.2017.05.065.

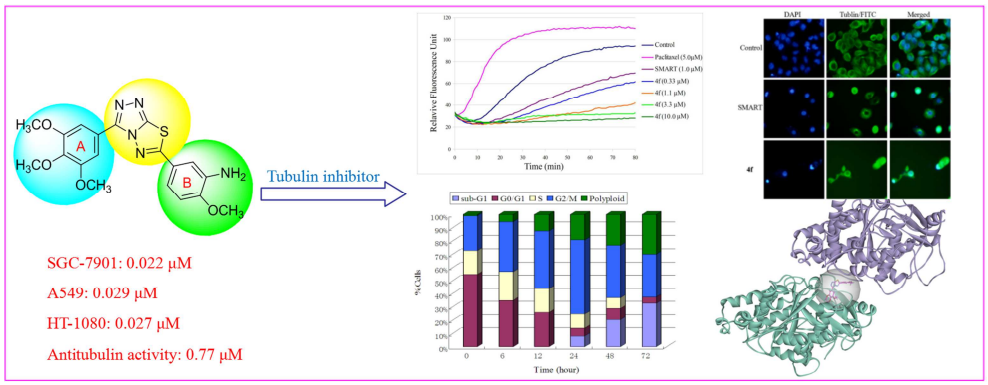

Design, synthesis and bioevaluation of antitubulin agents carrying diaryl-5,5-fused-heterocycle scaffold

Qile Xu,[a] Maolin Sun,[a] Zhaoshi Bai,[b] Yueting Wang,[a] Yue Wu,[a] Haiqiu Tian,[a] Daiying Zuo,[b] Qi Guan,[a] Kai Bao,[c]* Yingliang Wu[b]* and Weige Zhang[a]*

[a] Key Laboratory of Structure-Based Drug Design and Discovery, Ministry of Education, Shenyang Pharmaceutical University, 103 Wenhua Road, Shenhe District, Shenyang 110016, China.

[b] Department of Pharmacology, Shenyang Pharmaceutical University, 103 Wenhua Road, Shenhe District, Shenyang 110016, China.

[c] Wuya College of Innovation, Shenyang Pharmaceutical University, 103 Wenhua Road, Shenhe District, Shenyang 110016, China

* Corresponding authors:

E-mail addresses: zhangweige2000@sina.com (W. Zhang), yingliang_1016@163.com (Y. Wu), baokai@syphu.edu.cn (K. Bao).

Abstract

A series of 3,6-diaryl-1*H*-pyrazolo[5,1-c][1,2,4]triazoles (I) and 3,6-diaryl-[1,2,4]triazolo[3,4-b][1,3,4]thiadiazoles (II) as antitubulin agents were designed, synthesized and bioevaluated. Compounds (II) **4a, 4d, 4f, 4j, 4l** and **4n** showed potent antiproliferative activity at sub-micromolar or nanomolar concentrations against SGC-7901, A549 and HT-1080 cell lines, indicating that the bioisosteric replacement of the carbonyl group and B-ring of SMART and ABI with a 5,5-fused-heterocycle scaffold successfully maintained potent antiproliferative activity. Compound **4f** exhibited the most excellent antiproliferative activity against the three cancer cell lines (IC_{50} = 0.022-0.029 μM). Consistent with its potent antiproliferative activity, **4f** also displayed excellent antitubulin activity (IC_{50} = 0.77 μM). Furthermore, compound **4f** could dramatically affect cell morphology and microtubule networking, while cell cycle studies demonstrated that **4f** significantly induced SGC-7901cells arrest in G2/M phase. In addition, molecular docking studies supported the biological assay data and suggested that **4f** may be a potential antitubulin agent.

Keywords: Antiproliferative activity; Tubulin; Immunofluorescence; Cell cycle arrest; Molecular modeling

1. Introduction

Microtubule is one of the most attractive targets for anticancer drugs discovery [1]. Paclitaxel, vinblastine and colchicine represent the well-known microtubule targeting agents by binding three different binding sites (taxane, vinca and colchicine sites) of tubulin [1-3]. These agents interfere with the dynamic equilibrium of microtubules by either inhibition of tubulin polymerization or promotion the polymerization of tubulin, and both effects lead to the cell cycle arrest and limit cell proliferation thus resulting in cell death [1,4]. Given the tremendously successful clinical use of taxanes and vinca alkaloids, the colchicine binding site inhibitors (CBSIs) have aroused great interest among medicinal chemists [5-10].

Several outstanding CBSIs, such as 4-substituted methoxybenzoyl-aryl-thiazole (SMART **1**, Figure 1) and 2-aryl-4-benzoyl-imidazole (ABI **2**, Figure 1), exhibit potent antiproliferative activity, which contain three aromatic rings (A, B and C) and a carbonyl group between ring-A and ring-B [11,12]. Ring-closing is one strategy of bioisosterism in medicinal chemistry and represents a widely used method for rational design of new drugs [13,14]. Indeed, by applying this strategy, medicinal chemists successfully discovered some bioactive molecules including CBSIs [15,16]. Thus, we attempt to use the ring-closing strategy to design a series of new CBSIs carrying fused heterocyclic scaffold, the bioisosteres of the carbonyl group and B-ring (Figure 1). The target compounds were classified into the following two groups according to the 5,5-fused-heterocycle scaffold: (I) pyrazolo[5,1-c][1,2,4]triazole (**3a-e**), (II) [1,2,4]triazolo[3,4-b][1,3,4]thiadiazole (**4a-p**).

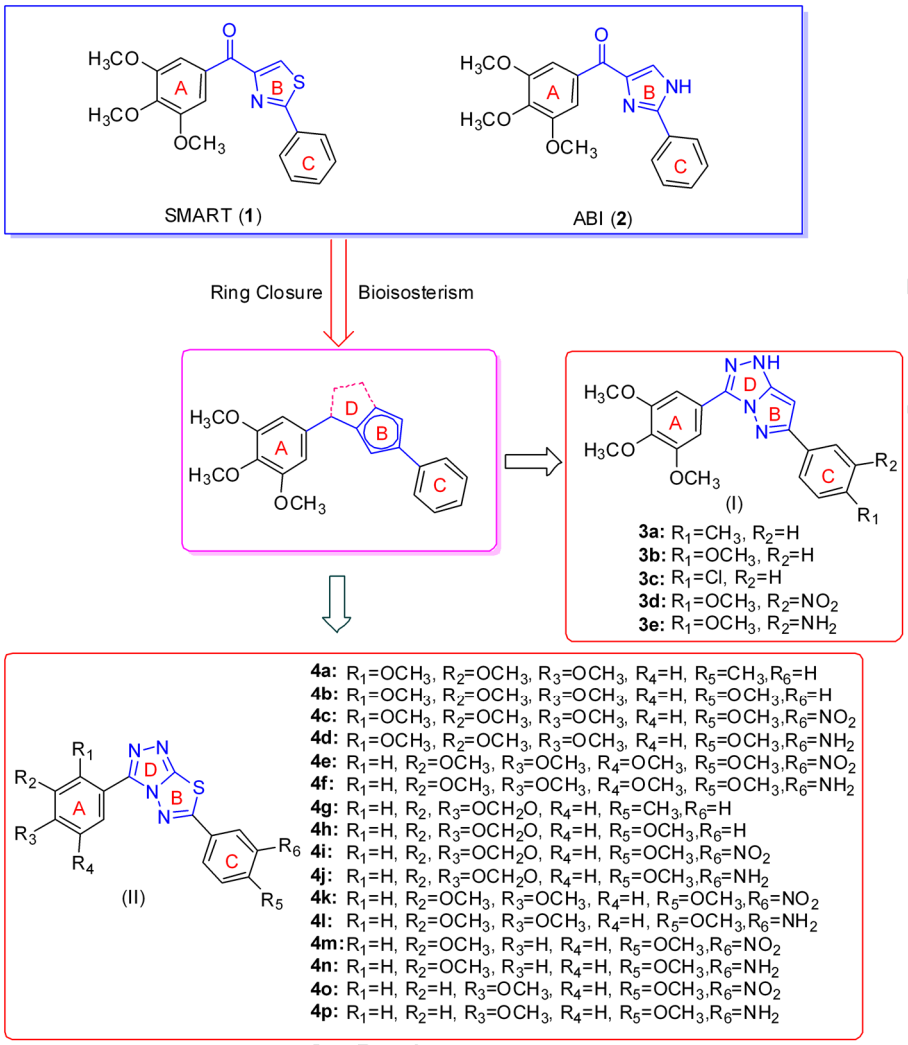

Figure 1. Design strategy and structures of new tubulin inhibitors

In view of the structural characteristics of SMART and ABI, we suspected that a certain angle∠ABC and distance between A and C (A, B and C represent the geometric center of ring-A, ring-B and ring-C, respectively) may necessary for the potent activity. In order to verify our speculation, calculation of the angle ABC and the distance between A and C of the skeletal structure of the target compounds, SMART and ABI, were performed with the Gaussian 09 software package. The angle and distance of compounds I were slightly larger than those of SMART and ABI, while the angle and distance of compounds II were pretty close to that of ABI (Figure 2). Herein, we describe the synthesis, bioevaluation and the preliminary structure-activity relationships of the 3,6-diaryl-[1,2,4]triazolo[3,4-b][1,3,4]thiadiazoles and

3,6-diaryl-1*H*-pyrazolo[5,1-c][1,2,4]triazoles as new antitubulin agents.

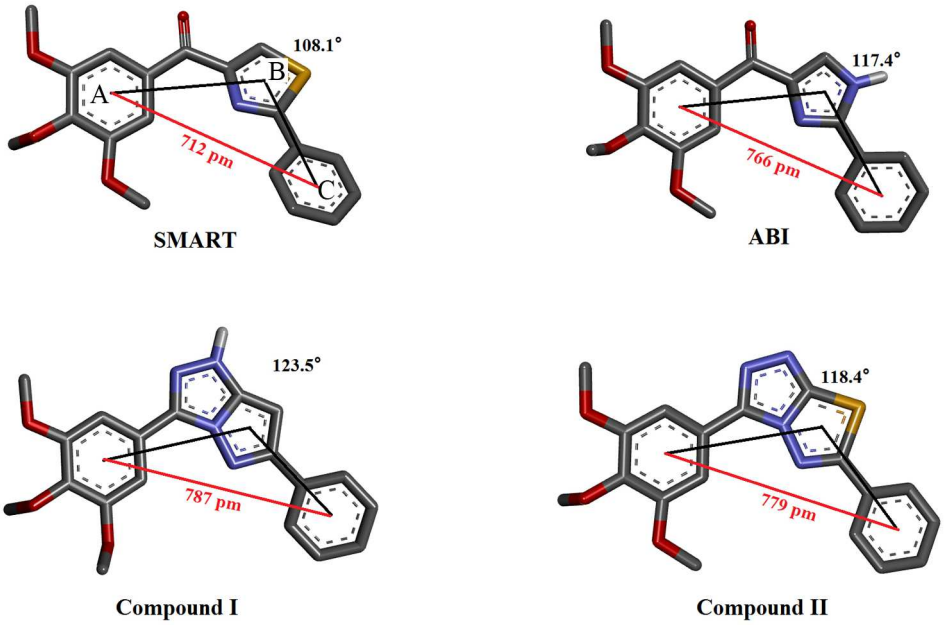

Figure 2. Caculation of∠ABC and distance between A and C of the SMART, ABI and the target compounds..

2. Results and discussion

2.1. Synthesis

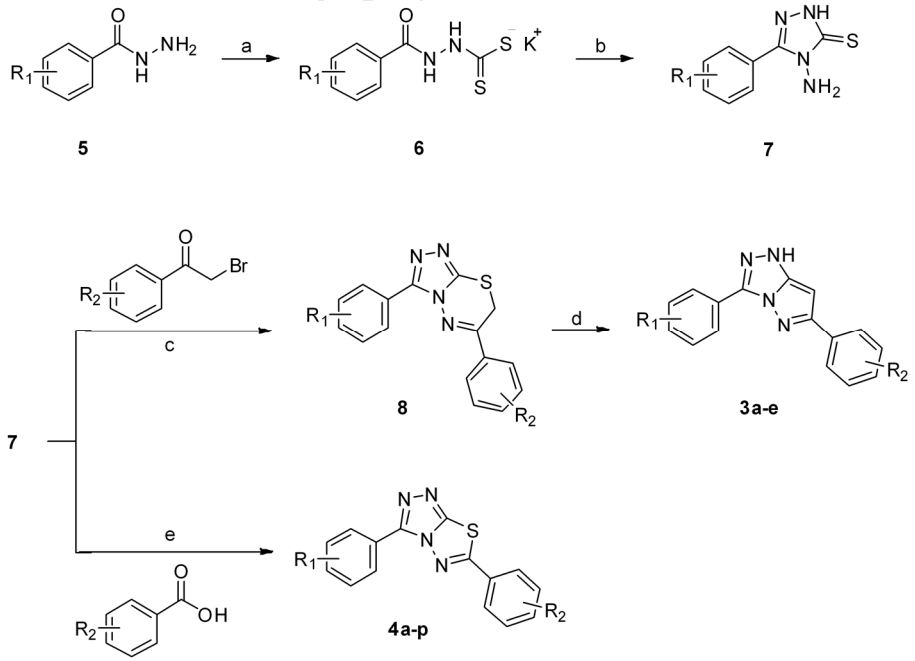

Figure 3. Reagents and conditions: (a) CS_2, KOH, MeOH, 25 °C; (b) $N_2H_4{\cdot}H_2O$, H_2O, MW, 100 °C; (c) EtOH, MW, 80 °C; (d) (i) Ac_2O, reflux, (ii) HCl, MeOH, reflux; (e) $POCl_3$, reflux.

The target compounds **3a-e** and **4a-p** were synthesized according to the synthetic route outlined in Figure 3. The hydrazides **5** were reacted with carbon disulphide and potassium hydroxide in methanol to afford corresponding dithiocarbazinates **6** and then underwent ring closure with an excess of 80% hydrazine monohydrate to give the key intermediate aryl triazoles **7** [17]. Then the aryl triazoles **7** were treated with α-bromoacetophenones to give the compounds **8** in ethanol under microwave irradiation (150 W, 80 °C). Compounds **8** were converted into the corresponding target compounds **3a-e** via desulfurization ring contraction [18]. On the other hand, a mixture of compounds **7** and substituted benzoic acids in phosphorus oxychloride was heated to reflux to get target compounds **4a-p**.

2.2. In vitro antiproliferative activity

The antiproliferative activities of target compounds **3a-e** and **4a-p** were evaluated against three human cancer cell lines (gastric adenocarcinoma SGC-7901 cells, lung adenocarcinoma A549 cells and fibrosarcoma HT-1080 cells) using MTT assay with SMART (**1**) and ABI (**2**) as reference. SMART (**1**) and ABI (**2**) gave IC_{50} values of 0.019-0.029, 0.15-0.98 μM, respectively. As depicted in Table 1, six target compounds (**4a**, **4d**, **4f**, **4j**, **4l** and **4n**) showed potent antiproliferative activity at sub-micromolar or nanomolar concentrations against the three different cancer cells. The angle and distance of 3,6-diaryl-[1,2,4]triazolo[3,4-b][1,3,4]thiadiazoles (118.4º, 779 pm) were more close to that of ABI (117.4º, 766 pm) than 3,6-diaryl-1H-pyrazolo[5,1-c][1,2,4]triazoles (123.5º, 787 pm) and the results of in vitro antiproliferative activity showed that compounds II were more active than compounds I. Compounds **3a-e** with a pyrazolo[5,1-c][1,2,4]triazole moiety displayed only modest antiproliferative activity. Replacement of the pyrazolo[5,1-c][1,2,4]triazole scaffold with the [1,2,4]triazolo[3,4-b][1,3,4]thiadiazole tended to greatly enhance the activity (**3d** vs **4e**, **3e** vs **4f**). When ring-A was a 2,3,4-trimethoxyphenyl moiety, compound **4d** with a 3-amino-4-methoxyphenyl group as ring-C exhibited the most active antiproliferative activity (0.062-0.082 μM). However, the 3-nitro-4-methoxy-substituted **4c** displayed a dramatic decrease in its antiproliferative activity. Compounds **4e**, **4i**, **4k**, **4m** and **4o** with a nitro group at

ring-C displayed similar antiproliferative activity with **4c**, suggesting that the electron-withdrawing nitro group is disfavored. Using 3-amino-4-methoxy substituents at ring-C, we examined the cytotoxic effect of compounds **4f**, **4j**, **4l**, **4n** and **4p** by replacement of 2,3,4-trimethoxy substituents with other substituents (3,4,5-trimethoxy, 3,4-methylenedioxy, 3,4-dimethoxy, 3-methoxy, 4-methoxy) at ring-A. These compounds (**4f**, **4j**, **4l** and **4n**) also showed potent antiproliferative activity and broaden the SAR by modifications on ring-C. 3,4,5-Trimethoxy-substituted compound **4f** exhibited the most excellent antiproliferative activity against the three cancer cell lines (IC_{50} = 0.022-0.029 μM), which was comparable to SMART (IC_{50} = 0.019-0.029 μM) but more effective than ABI (IC_{50} = 0.15-0.98 μM).

Table 1. Antiproliferative activity of **3a-e**, **4a-p**, SMART and ABI.

Compd	Antiproliferative activity (IC_{50}± SD, μM) [a]		
	SGC-7901	A549	HT-1080
3a	33.5 ± 1.9	29.3 ± 1.2	51.3 ± 2.6
3b	26.8 ± 1.1	26.4 ± 2.0	26.5 ± 2.2
3c	6.12 ± 0.13	1.21 ± 0.09	6.81 ± 0.21
3d	48.3 ± 1.5	58.2 ± 2.9	35.6 ± 3.8
3e	13.8 ± 1.6	17.4 ± 2.0	17.8 ± 1.5
4a	**0.186 ± 0.012**	**0.803 ± 0.021**	**0.089 ± 0.008**
4b	3.75 ± 0.02	2.29 ± 0.09	1.88 ± 0.05
4c	32.5 ± 1.2	33.8 ± 1.4	35.1 ± 1.5
4d	**0.062 ± 0.007**	**0.082 ± 0.008**	**0.073 ± 0.016**
4e	23.2 ± 1.3	26.5 ± 2.1	30.2 ± 1.2
4f	**0.022 ± 0.006**	**0.029 ± 0.011**	**0.027 ± 0.013**
4g	24.0 ± 1.4	27.7 ± 0.9	26.8 ± 1.3
4h	25.6 ± 2.1	29.7 ± 1.7	24.5 ± 0.8
4i	37.8 ± 3.1	32.8 ± 2.5	30.3 ± 3.0
4j	**0.057 ± 0.011**	**0.272 ± 0.007**	**0.327 ± 0.018**
4k	37.7 ± 1.6	30.4 ± 1.7	32.8 ± 2.1
4l	**0.083 ± 0.009**	**0.522 ± 0.021**	**0.339 ± 0.032**
4m	34.7 ± 2.4	29.5 ± 0.5	33.0 ± 0.8

4n	**0.059 ± 0.004**	**0.12 ± 0.06**	**0.088 ± 0.017**
4o	22.1 ± 0.7	26.9 ± 1.9	27.3 ± 1.4
4p	14.2 ± 1.1	14.9 ± 0.9	16.4 ± 1.5
SMART (**1**) [b]	0.019 ± 0.008	0.029 ± 0.009	0.028 ± 0.011
ABI (**2**) [b]	0.81 ± 0.08	0.98 ± 0.11	0.15 ± 0.05

[a] IC_{50}: the half maximal inhibitory concentration. [b] Used as positive controls.

2.3. Tubulin polymerization

To explore the relationship between the antiproliferative activities of these compounds and tubulin, compound **4f** was evaluated for its effects on tubulin polymerization in comparison to the positive control SMART (**1**) and the negative control paclitaxel. As shown in Figure 4, **4f** significantly inhibited tubulin polymerization (IC_{50}: 0.77 μM) which was different from the negative control paclitaxel. Furthermore, compound **4f** inhibited tubulin polymerization in a dose-dependent manner. These results suggested that the molecular target of this series of compounds was most likely tubulin.

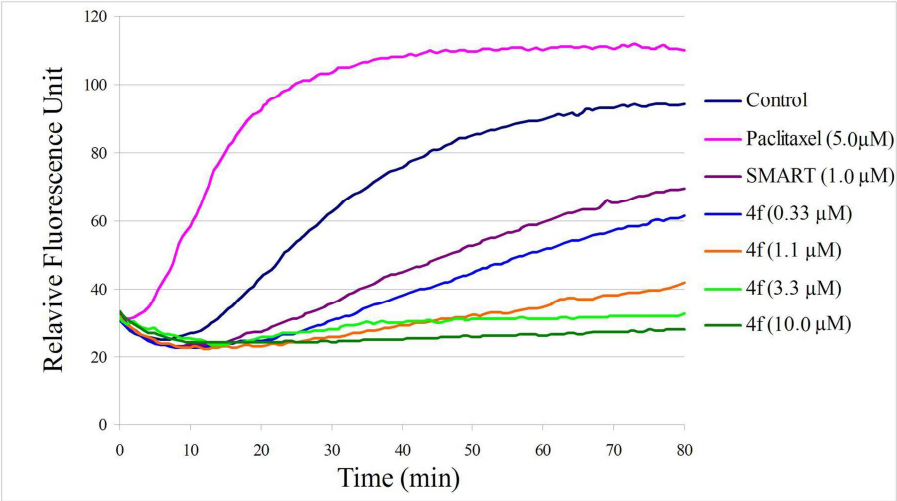

Figure 4. Effects of **4f** on tubulin polymerization. Tubulin had been pre-incubated for 1 min with **4f** (0.33 μM, 1.1 μM, 3.3 μM and 10.0 μM), SMART (1.0 μM), paclitaxel (5.0 μM) or vehicle DMSO (control) before GTP was added to start the tubulin polymerization reactions. Polymerization of microtubule was monitored kinetically by using a spectrophotometer.

2.4. Analysis of immunofluorescence staining

To confirm the direct effects of compound **4f** on tubulin, we further investigated alterations in the microtubule network induced by **4f** and SMART (**1**) in cultured

SGC-7901 cells using immunofluorescence techniques. As given in Figure 5, the microtubule network without drug treatment displays normal arrangement and organization in control cells. Whereas SGC-7901 cells were treated with compound **4f** or SMART (at their 2-fold IC_{50} concentrations, respectively) and the results demonstrated that microtubules became short and wrapped around the nucleus in comparison with the control. These results indicated that **4f** similar to SMART could destabilize microtubules.

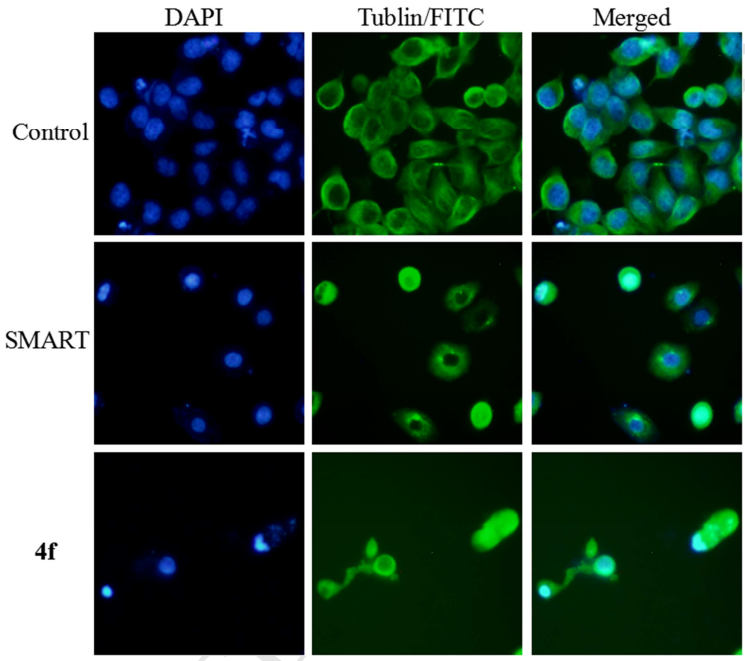

Figure 5. Effects of **4f** on tubulin assembly in SGC-7901 cells by immunofluorescence assay. SGC-7901 cells were treated with DMSO (control), **4f** (0.044 μM) or SMART (0.038 μM) for 48 h.

2.5. Cell cycle study

Because most tubulin inhibitors induce cell cycle arrest in the G2/M phase [19], we next investigated the time-effects on cell cycle distribution of SGC-7901cells treated with **4f** (2-fold IC_{50}) by flow cytometry. As given in Figure 6, as time went on, compound **4f** was found to significantly increase the percentage of cells in the sub-G1 and G2/M phases, with an accompanying decrease in cells in the G0/G1 and S phases. The biggest percentage of G2/M phase appeared after the cells were treated with compound **4f** for 24 h. At the same time, polyploidy was induced increasingly by **4f**. Thus, cell cycle studies demonstrated that **4f** significantly induced SGC-7901cells

arrest in G2/M phase in a time-dependent manner (Figure S1).

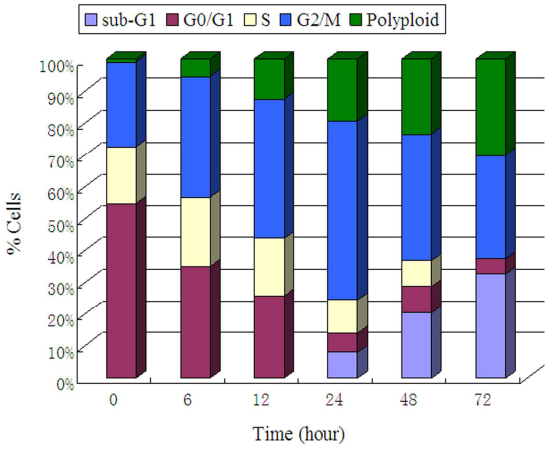

Figure 6. The statistical graph of cell cycle distribution. Cell cycle distribution of SGC-7901 cells treated for 0, 6, 12, 24, 48, 72 h with **4f** (0.044 μM).

2.6. Molecular modeling study

To further understand the binding interactions, molecular docking studies of **4f** was carried out with tubulin crystal structure (PDB: 1SA0) using the CDOCKER program of Discovery Studio 3.0 software. As given in Figure 7, the 3,4,5-trimethoxybenzoyl ring-A of **4f** was located deeply into the β-subunit of tubulin. The ring-B and ring-C of **4f** extends toward the α/β-tubulin interface and several important amino acids of tubulin formed hydrogen bond interactions with **4f**. The residue of β-Cys241 forms a hydrogen bond with the oxygen of the methoxy group (ring-A). Furthermore, sulfur atom of ring-B forms a hydrogen bond with the residue β-Asn101. These molecular docking results further supported the above biological assay data and suggested that **4f** may be a potential tubulin inhibitor.

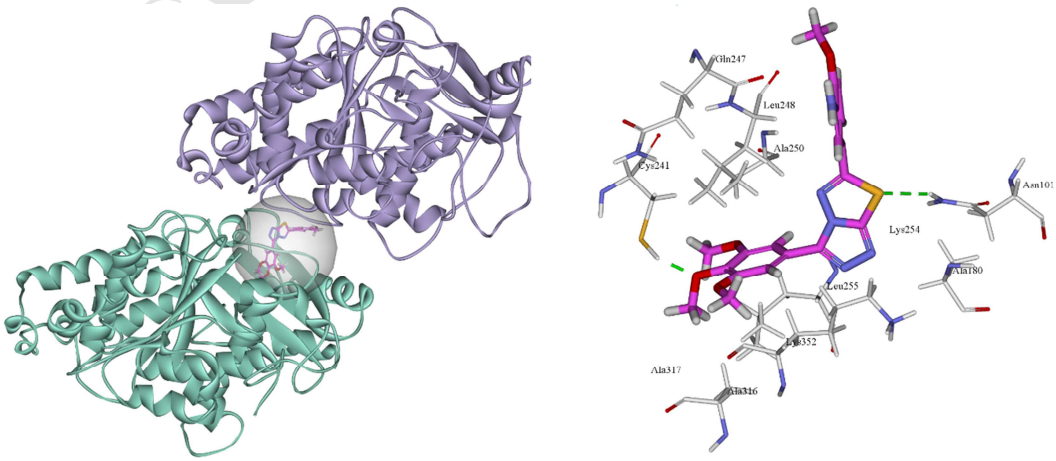

Figure 7. The binding mode of compound **4f** in the colchicine binding site of tubulin (left). Overlay of **4f** in the binding site (right).

3. Conclusions

A series of new tubulin inhibitors with a 5,5-fused-heterocycle scaffold were designed and synthesized as the analogs of SMART and ABI. We proposed the two parameters of angle∠ABC and distance between A and C to examine the relationship between the designed compounds and the lead compounds. The angle and distance of 3,6-diaryl-[1,2,4]triazolo[3,4-b][1,3,4]thiadiazoles were more close to that of ABI (117.4º, 766 pm) than 3,6-diaryl-1*H*-pyrazolo[5,1-c][1,2,4]triazoles, and SAR studies indicated that compounds with a [1,2,4]triazolo[3,4-b][1,3,4]thiadiazole scaffold were more potent than those with the pyrazolo[5,1-c][1,2,4]triazole scaffold. Six target compounds (**4a, 4d, 4f, 4j, 4l and 4n**) showed potent antiproliferative activity at sub-micromolar or nanomolar concentrations against the three different cancer cells, indicating that the bioisosteric replacement of the carbonyl group and ring-B of SMART and ABI with a 5,5-fused-heterocycle scaffold successfully maintained potent antiproliferative activity. Compound **4f** exhibited the most excellent antiproliferative activity against the three cancer cell lines, which was comparable to SMART but more effective than ABI. Consistent with its potent antiproliferative activity, **4f** also displayed excellent antitubulin activity with an IC_{50} value of 0.77 μM. Furthermore, compound **4f** could significantly affect cell morphology and microtubule networking and cell cycle studies demonstrated that **4f** significantly induced SGC-7901cells arrest in G2/M phase. Molecular docking studies suggested that **4f** may be a potential tubulin inhibitor.

4. Experimental Section

4.1. Chemistry

All reagents and solvents were obtained from commercially available sources and were used without purification. The microwave reactions were performed on a

discover-sp single mode microwave reactor from CEM Corporation. Reactions were monitored by TLC with silica gel plates under UV light (λ = 254 nm). The melting points (uncorrected) were measured on a hot-stage microscope (X-4, Beijing Taike Ltd.). ^{1}H NMR and ^{13}C NMR spectra were obtained on a Bruker AVANCE 300 or 600 in $CDCl_3$ or DMSO-d_6 (TMS as internal standard). Mass spectra (MS) were measured on an Agilent 1100-sl mass spectrometer with an electrospray ionization source from Agilent Co. Ltd.

*4.1.2. General synthetic procedure for the key intermediates **7**.*

The substituted hydrazides **5** (10 mmol) were stirred with potassium hydroxide (15 mmol) in absolute methanol. Then CS_2 (12 mmol) was slowly added and the mixture was stirred at 25 °C for 1-6 h. After the reaction completed, the solid was precipitated and dried to afford compounds **6**. The compounds **6** was refluxed with excess 80% hydrazine hydrate in water under microwave irradiation at 250 W, 100 °C, for 60 min. After completion of the reaction, the mixture was acidified with concentrated HCl and the precipitate solid was filtered, washed with water, dried and recrystallized from aqueous methanol to obtain the intermediates **7**.

*4.1.3. General synthetic procedures for **3a-e**.*

To a mixture of each of intermediates **7** (10 mmol) in absolute ethylalcohol (15 mL), was added the appropriate α-haloketones (10 mmol). The mixture was heated at 80 °C under microwave irradiation until the reaction was complete. Water was added and the precipitate **8** formed was collected. Then compounds **8** were added slowly to acetic anhydride and the mixture was refluxed for 4 h. Then the mixture was poured into cold water. Precipitated solid was filtered, washed with water and dried. Finally, the precipitated solid was added to a mixture of methanol (30 mL) and HCl (4 mL, 10 M) and the mixture was refluxed for 6–24 h. Finally, the solvent was removed in vacuo and the remaining materials were washed with sodium bicarbonate solution and the remaining materials were recrystallized from the proper solvent.

*4.1.4. General synthetic procedures for **4a-p**.*

A mixture of intermediates **7** (4 mmol) and substituted benzoic acid (4 mmol) in phosphorus oxychloride (10 mL) was heated under reflux for 2 h [20]. After the

reaction completed, the solution was poured into 200g of ice. Precipitate was filtered, washed with water and recrystallized from the proper solvent.

4.1.5.

*3-(3,4,5-Trimethoxyphenyl)-6-(4-methylphenyl)-1H-pyrazolo[5,1-c][1,2,4]triazole (**3a**).*

Brown solid; yield: 81%; M.p.: 119-122 ^{o}C; ^{1}H-NMR (600 MHz, $CDCl_3$): δ 9.73 (s, 1H), 7.88 (s, 2H), 7.82 (d, *J* = 8.0 Hz, 2H), 7.25 (d, *J* = 8.0 Hz, 2H), 6.02 (s, 1H), 4.01 (s, 6H), 3.94 (s, 3H), 2.40 (s, 3H); ^{13}C-NMR (150 MHz, $CDCl_3$): δ 160.1, 153.4 (2C), 148.4, 139.5, 139.4, 138.4, 130.9, 129.3 (2C), 126.0 (2C), 121.1, 103.8 (2C), 75.0, 60.9, 56.2 (2C), 21.3; ESI-MS: m/z = 365.3 $[M+H]^+$, 387.3 $[M+Na]^+$.

4.1.6.

*3-(3,4,5-Trimethoxyphenyl)-6-(4-methoxyphenyl)-1H-pyrazolo[5,1-c][1,2,4]triazole (**3b**).*

Red solid; yield: 84%; M.p.: 146-147 ^{o}C; ^{1}H-NMR (600 MHz, $CDCl_3$): δ 9.89 (s, 1H), 7.87 (s, 2H), 7.86 (d, *J* = 8.7 Hz, 2H), 6.97 (d, *J* = 8.7 Hz, 2H), 5.99 (s, 1H), 4.01 (s, 6H), 3.93 (s, 3H), 3.86 (s, 3H); ^{13}C-NMR (150 MHz, $CDCl_3$): δ 159.9, 159.8, 153.4 (2C), 148.4, 139.5, 139.3, 127.3 (2C), 126.5, 121.2, 114.0 (2C), 103.8 (2C), 74.6, 60.9, 56.2 (2C), 55.3; ESI-MS: m/z = 381.3 $[M+H]^+$.

4.1.7.

*3-(3,4,5-Trimethoxyphenyl)-6-(4-chlorophenyl)-1H-pyrazolo[5,1-c][1,2,4]triazole (**3c**).*

Red solid; yield: 82%; M.p.: 150-151 ^{o}C; ^{1}H-NMR (600 MHz, $CDCl_3$): δ 9.65 (s, 1H), 7.86 (s, 2H), 7.85 (d, *J* = 8.4 Hz, 2H), 7.41 (d, *J* = 8.4 Hz, 2H), 6.05 (s, 1H), 4.02 (s, 6H), 3.94 (s, 3H); ^{13}C-NMR (150 MHz, $CDCl_3$): δ 158.7, 153.4 (2C), 148.4, 139.7, 139.4, 134.3, 132.3, 128.8 (2C), 127.3 (2C), 120.9, 103.8 (2C), 75.3, 60.9, 56.2 (2C); ESI-MS: m/z = 385.0 $[M+H]^+$, 407.1 $[M+Na]^+$.

4.1.8.

*3-(3,4,5-Trimethoxyphenyl)-6-(3-nitro-4-methoxyphenyl)-1H-pyrazolo[5,1-c][1,2,4]triazole (**3d**).*

Yellow solid; yield: 76%; M.p.: 149-151 ^{o}C; ^{1}H-NMR (400 MHz, DMSO-d_6): δ 13.24

(s, 1H), 8.41 (d, *J* = 2.0 Hz, 1H), 8.25 (dd, *J* = 8.8 Hz, *J* = 2.0 Hz, 1H), 7.80 (s, 2H), 7.44 (d, *J* = 8.8 Hz, 1H), 6.50 (s, 1H), 3.97 (s, 3H), 3.93 (s, 6H), 3.76 (s, 3H); ^{13}C-NMR (100 MHz, DMSO-d_6): δ 156.7, 153.7 (2C), 152.3, 149.2, 139.9, 139.4, 137.8, 131.7, 126.9, 122.3, 121.5, 115.2, 103.6 (2C), 75.7, 60.7, 57.3, 56.4 (2C); ESI-MS: m/z = 426.1 $[M+H]^+$, 448.1 $[M+Na]^+$.

4.1.9.

*3-(3,4,5-Trimethoxyphenyl)-6-(3-amino-4-methoxyphenyl)-1H-pyrazolo[5,1-c][1,2,4]triazole (**3e**).*

Brown solid; yield: 69%; M.p.: 135-137 ^{o}C; ^{1}H-NMR (600 MHz, $CDCl_3$): δ 9.86 (s, 1H), 7.85 (s, 2H), 7.31 (s, 2H), 6.84 (d, *J* = 8.8 Hz, 1H), 5.95 (s, 1H), 4.00 (s, 6H), 3.92 (s, 3H), 3.89 (s, 3H); ^{13}C-NMR (150 MHz, $CDCl_3$): δ 160.2, 153.4 (2C), 148.3, 147.9, 139.5, 139.4, 135.9, 126.8, 121.2, 116.8, 112.9, 110.3, 103.8 (2C), 74.8, 60.9, 56.2 (2C), 55.5; ESI-MS: m/z = 396.4 $[M+H]^+$.

4.1.10.

*3-(2,3,4-Trimethoxyphenyl)-6-(4-methylphenyl)-[1,2,4]triazolo[3,4-b][1,3,4]thiadiazole (**4a**).*

White solid; yield: 72%; M.p.: 100-103 ^{o}C; ^{1}H-NMR (600 MHz, $CDCl_3$): δ 7.75 (d, *J* = 8.2 Hz, 2H), 7.52 (d, *J* = 8.6 Hz, 1H), 7.30 (d, *J* = 8.2 Hz, 2H), 6.82 (d, *J* = 8.6 Hz, 1H), 4.01 (s, 3H), 3.94 (s, 3H), 3.91 (s, 3H), 2.42 (s, 3H); ^{13}C-NMR (150 MHz, $CDCl_3$): δ 166.0, 156.0, 153.4, 152.5, 145.3, 143.4, 142.3, 130.0 (2C), 126.9 (2C), 126.8, 125.6, 112.5, 107.2, 61.6, 60.8, 56.1, 21.5; ESI-MS: m/z = 383.1 $[M+H]^+$.

4.1.11.

*3-(2,3,4-Trimethoxyphenyl)-6-(4-methoxyphenyl)-[1,2,4]triazolo[3,4-b][1,3,4]thiadiazole (**4b**).*

Brown solid; yield: 69%; M.p.: 112-114 ^{o}C; ^{1}H-NMR (600 MHz, $CDCl_3$): δ 7.69 (d, *J* = 8.7 Hz, 2H), 7.44 (d, *J* = 8.6 Hz, 1H), 6.88 (d, *J* = 8.7 Hz, 2H), 6.74 (d, *J* = 8.6 Hz, 1H), 3.93 (s, 3H), 3.85 (s, 3H), 3.84 (s, 3H), 3.76 (s, 3H); ^{13}C-NMR (150 MHz, $CDCl_3$): δ 165.4, 162.9, 155.8, 153.3, 152.4, 145.1, 142.2, 128.6 (2C), 125.4, 121.7, 114.6 (2C), 112.5, 107.2, 61.5, 60.7, 56.0, 55.4; ESI-MS: m/z = 399.1 $[M+H]^+$.

4.1.12.

*3-(2,3,4-Trimethoxyphenyl)-6-(3-nitro-4-methoxyphenyl)-[1,2,4]triazolo[3,4-b][1,3,4] thiadiazole (**4c**).*

White solid; yield: 75%; M.p.: 195-197 ^{o}C; ^{1}H-NMR (600 MHz, DMSO-d_6): δ 8.44 (d, *J* = 2.4 Hz, 1H), 8.22 (dd, *J* = 8.9 Hz, *J* = 2.4 Hz, 1H), 7.57 (d, *J* = 8.9 Hz, 1H), 7.45 (d, *J* = 8.6 Hz, 1H), 7.02 (d, *J* = 8.6 Hz, 1H), 4.03 (s, 3H), 3.90 (s, 6H), 3.82 (s, 3H); ^{13}C-NMR (150 MHz, DMSO-d_6): δ 164.4, 156.3, 155.1, 153.6, 152.2, 144.7, 142.2, 140.0, 133.1, 125.9, 124.0, 121.6, 115.9, 112.1, 108.5, 61.9, 60.9, 57.8, 56.5; ESI-MS: m/z = 444.1 $[M+H]^+$, 466.1 $[M+Na]^+$.

4.1.13.

*3-(2,3,4-Trimethoxyphenyl)-6-(3-amino-4-methoxyphenyl)-[1,2,4]triazolo[3,4-b][1,3, 4]thiadiazole (**4d**).*

Yellow solid; yield: 66%; M.p.: 139-142 ^{o}C; ^{1}H-NMR (600 MHz, DMSO-d_6): δ 7.40 (d, *J* = 8.6 Hz, 1H), 7.23 (d, *J* = 2.3 Hz, 1H), 7.11 (dd, *J* = 8.4 Hz, *J* = 2.3 Hz, 1H), 7.01 (d, *J* = 8.6 Hz, 1H), 6.95 (d, *J* = 8.4 Hz, 1H), 5.20 (s, 2H), 3.90 (s, 3H), 3.90 (s, 3H), 3.85 (s, 3H), 3.83 (s, 3H); ^{13}C-NMR (150 MHz, DMSO-d_6): δ 166.8, 156.1, 153.1, 152.2, 150.3, 144.7, 142.2, 139.2, 125.9, 121.9, 116.3, 112.7, 111.0, 110.7, 108.4, 61.9, 60.9, 56.5, 56.0; ESI-MS: m/z = 414.3 $[M+H]^+$, 436.3 $[M+Na]^+$.

4.1.14.

*3-(3,4,5-Trimethoxyphenyl)-6-(3-nitro-4-methoxyphenyl)-[1,2,4]triazolo[3,4-b][1,3,4] thiadiazole (**4e**).*

Yellow solid; yield: 65%; M.p.: 246-248 ^{o}C; ^{1}H-NMR (600 MHz, DMSO-d_6): δ 8.49 (s, 1H), 8.26 (d, *J* = 8.5 Hz, 1H), 7.58 (d, *J* = 8.8 Hz, 1H), 7.55 (s, 2H), 4.04 (s, 3H), 3.90 (s, 6H), 3.76 (s, 3H); ^{13}C-NMR (150 MHz, DMSO-d_6): δ 165.0, 155.2, 153.7, 153.7 (2C), 139.9, 139.6, 133.2, 124.3, 121.5, 121.0, 116.1, 103.7 (2C), 103.0, 60.6, 57.8, 56.3 (2C); ESI-MS: m/z = 444.1 $[M+H]^+$, 466.1 $[M+Na]^+$.

4.1.15.

*3-(3,4,5-Trimethoxyphenyl)-6-(3-amino-4-methoxyphenyl)-[1,2,4]triazolo[3,4-b][1,3, 4]thiadiazole (**4f**).*

White solid; yield: 61%; M.p.: 153-155 ^{o}C; ^{1}H-NMR (600 MHz, DMSO-d_6): δ 7.56 (s, 2H), 7.24 (s, 1H), 7.17 (d, *J* = 7.8 Hz, 1H), 6.97 (d, *J* = 8.2 Hz, 1H), 5.25 (s, 2H), 3.90

(s, 6H), 3.86 (s, 3H), 3.76 (s, 3H); ^{13}C-NMR (150 MHz, DMSO-d_6): δ 167.6, 153.9, 153.6 (2C), 150.4, 145.5, 139.4, 139.2, 121.8, 121.2, 116.3, 111.0, 110.8, 103.6 (2C), 60.6, 56.4 (2C), 56.0 ; ESI-MS: m/z = 414.1 $[M+H]^+$, 436.1 $[M+Na]^+$.

4.1.16.

*3-(3,4-Methylenedioxyphenyl)-6-(4-methylphenyl)-[1,2,4]triazolo[3,4-b][1,3,4]thiadiazole (**4g**).*

White solid; yield: 69%; M.p.: 162-165 ^{o}C; ^{1}H-NMR (600 MHz, $CDCl_3$): δ 7.96 (dd, *J* = 8.2 Hz, *J* = 1.4 Hz, 1H), 7.86 (d, *J* = 1.4 Hz, 1H), 7.80 (d, *J* = 8.1 Hz, 2H), 7.33 (d, *J* = 8.1 Hz, 2H), 6.97 (d, *J* = 8.2 Hz, 1H), 6.06 (s, 2H), 2.45 (s, 3H); ^{13}C-NMR (150 MHz, $CDCl_3$): δ 166.7, 153.8, 149.3, 148.0, 146.4, 143.6, 130.1 (2C), 127.0 (2C), 126.6, 121.0, 119.6, 108.7, 106.7, 101.5, 21.6; ESI-MS: m/z = 337.1 $[M+H]^+$, 359.0 $[M+Na]^+$.

4.1.17.

*3-(3,4-Methylenedioxyphenyl)-6-(4-methoxyphenyl)-[1,2,4]triazolo[3,4-b][1,3,4]thiadiazole (**4h**).*

White solid; yield: 74%; M.p.: 145-147 ^{o}C; ^{1}H-NMR (600 MHz, $CDCl_3$): δ 7.92 (dd, *J* = 8.1 Hz, *J* = 1.3 Hz, 1H), 7.82-7.83 (m, 3H), 6.99 (d, *J* = 8.8 Hz, 2H), 6.94 (d, *J* = 8.1 Hz, 1H), 6.03 (s, 2H), 3.87 (s, 3H); ^{13}C-NMR (150 MHz, $CDCl_3$): δ 166.3, 163.1, 154.0, 149.3, 148.0, 146.3, 128.8 (2C), 121.7, 121.0, 119.6, 114.8 (2C), 108.6, 106.7, 101.5, 55.6; ESI-MS: m/z = 353.1 $[M+H]^+$, 375.0 $[M+Na]^+$.

4.1.18.

*3-(3,4-Methylenedioxyphenyl)-6-(3-nitro-4-methoxyphenyl)-[1,2,4]triazolo[3,4-b][1,3,4]thiadiazole (**4i**).*

White solid; yield: 65%; M.p.: 135-137 ^{o}C; ^{1}H-NMR (600 MHz, DMSO-d_6): δ 8.56 (s, 1H), 8.29 (d, *J* = 8.7 Hz, 1H), 7.88 (d, *J* = 7.9 Hz, 1H), 7.74 (s, 1H), 7.59 (d, *J* = 8.9 Hz, 1H), 7.16 (d, *J* = 8.1 Hz, 1H), 6.16 (s, 2H), 4.05 (s, 3H); ^{13}C-NMR (150 MHz, DMSO-d_6): δ 164.9, 155.0, 150.8, 149.4, 148.3, 145.2, 140.1, 133.3, 124.0, 121.5, 121.1, 119.5, 115.8, 109.3, 106.3, 102.2, 56.4; ESI-MS: m/z = 398.3 $[M+H]^+$, 420.3 $[M+Na]^+$.

4.1.19.

*3-(3,4-Methylenedioxyphenyl)-6-(3-amino-4-methoxyphenyl)-[1,2,4]triazolo[3,4-b][1,3,4]thiadiazole (**4j**).*

Yellow solid; yield: 56%; M.p.: 182-185 ^{o}C; ^{1}H-NMR (600 MHz, DMSO-d_6): δ 7.85 (dd, *J* = 8.2 Hz, *J* = 1.7 Hz, 1H), 7.74 (d, *J* = 1.7 Hz, 1H), 7.31 (d, *J* = 2.3 Hz, 1H), 7.19 (dd, *J* = 8.3 Hz, *J* = 2.3 Hz, 1H), 7.17 (d, *J* = 8.2 Hz, 1H), 6.99 (d, *J* = 8.3 Hz, 1H), 6.16 (s, 2H), 3.87 (s, 3H); ^{13}C-NMR (150 MHz, DMSO-d_6): δ 167.6, 153.8, 150.5, 149.3, 148.2, 145.6, 139.2, 121.8, 120.9, 119.8, 116.6, 111.0, 110.8, 109.3, 106.3, 102.1, 56.0; ESI-MS: m/z = 368.1 $[M+H]^+$.

4.1.20.

*3-(3,4-Dimethoxyphenyl)-6-(3-nitro-4-methoxyphenyl)-[1,2,4]triazolo[3,4-b][1,3,4]thiadiazole (**4k**).*

Yellow solid; yield: 67%; M.p.: 136-139 ^{o}C; ^{1}H-NMR (600 MHz, DMSO-d_6): δ 8.53 (d, *J* = 2.2 Hz, 1H), 8.28 (dd, *J* = 8.8 Hz, *J* = 2.2 Hz, 1H), 7.92 (dd, *J* = 8.5 Hz, *J* = 1.9 Hz, 1H), 7.78 (d, *J* = 1.9 Hz, 1H), 7.59 (d, *J* = 9.0 Hz, 1H), 7.18 (d, *J* = 8.5 Hz, 1H), 4.05 (s, 3H), 3.89 (s, 3H), 3.85 (s, 3H); ^{13}C-NMR (150 MHz, DMSO-d_6): δ 164.7, 155.1, 154.0, 150.9, 149.3, 145.9, 140.0, 133.2, 124.0, 121.5, 119.4, 118.2, 115.9, 112.3, 109.2, 57.8, 56.0, 55.9; ESI-MS: m/z = 414.1 $[M+H]^+$, 436.3 $[M+Na]^+$.

4.1.21.

*3-(3,4-Dimethoxyphenyl)-6-(3-amino-4-methoxyphenyl)-[1,2,4]triazolo[3,4-b][1,3,4]thiadiazole (**4l**).*

Pale yellow solid; yield: 59%; M.p.: 160-162 ^{o}C; ^{1}H-NMR (600 MHz, DMSO-d_6): δ 7.88 (dd, *J* = 8.4 Hz, *J* = 1.9 Hz, 1H), 7.79 (d, *J* = 1.9 Hz, 1H), 7.28 (d, *J* = 2.3 Hz, 1H), 7.19 (dd, *J* = 8.2 Hz, *J* = 2.3 Hz, 1H), 7.17 (d, *J* = 8.4 Hz, 1H), 6.98 (d, *J* = 8.2 Hz, 1H), 5.24 (s, 2H), 3.89 (s, 3H), 3.87 (s, 3H), 3.85 (s, 3H); ^{13}C-NMR (150 MHz, DMSO-d_6): δ 167.4, 153.7, 150.8, 150.4, 149.3, 145.7, 139.2, 121.9, 119.3, 118.5, 116.4, 112.2, 111.0, 110.9, 109.3, 56.0, 56.0, 55.9; ESI-MS: m/z = 384.4 $[M+H]^+$, 406.3 $[M+Na]^+$.

4.1.22.

*3-(3-Methoxyphenyl)-6-(3-nitro-4-methoxyphenyl)-[1,2,4]triazolo[3,4-b][1,3,4]thiadiazole (**4m**).*

Pale yellow solid; yield: 76%; M.p.: 236-238 ^{o}C; ^{1}H-NMR (600 MHz, DMSO-d_6): δ 8.50 (d, *J* = 2.2 Hz, 1H), 8.25 (dd, *J* = 8.8 Hz, *J* = 2.2 Hz, 1H), 7.88 (d, *J* = 7.7 Hz, 1H), 7.77 (s, 1H), 7.57 (d, *J* = 8.8 Hz, 1H), 7.50-7.53 (m, 1H), 7.11 (dd, *J* = 8.2 Hz, *J* = 2.2 Hz, 1H), 4.04 (s, 3H), 3.85 (s, 3H); ^{13}C-NMR (150 MHz, DMSO-d_6): δ 165.1, 159.9, 155.1, 154.6, 145.7, 140.0, 133.3, 130.8, 126.9, 124.1, 121.5, 118.6, 116.5, 115.9, 111.4, 57.8, 56.4; ESI-MS: m/z = 384.1 $[M+H]^+$, 406.3 $[M+Na]^+$.

4.1.23.

*3-(3-Methoxyphenyl)-6-(3-amino-4-methoxyphenyl)-[1,2,4]triazolo[3,4-b][1,3,4]thia diazole (**4n**).*

Brown solid; yield: 69%; M.p.: 169-170 ^{o}C; ^{1}H-NMR (600 MHz, DMSO-d_6): δ 7.87 (d, *J* = 7.8 Hz, 1H), 7.80-7.81 (m, 1H), 7.51-7.54 (m, 1H), 7.29 (d, *J* = 2.3 Hz, 1H), 7.17 (dd, *J* = 8.3 Hz, *J* = 2.3 Hz, 1H), 7.13 (dd, *J* = 8.2 Hz, *J* = 2.5 Hz, 1H), 6.97 (d, *J* = 8.4 Hz, 1H), 5.25 (s, 2H), 3.87 (s, 3H), 3.86 (s, 3H); ^{13}C-NMR (150 MHz, DMSO-d_6): δ 167.8, 159.9, 150.5, 145.6, 139.2, 130.7, 130.6, 127.2, 121.8, 118.5, 116.5, 116.2, 111.4, 111.0, 110.8, 56.0, 55.7; ESI-MS: m/z = 354.4 $[M+H]^+$, 376.3 $[M+Na]^+$.

4.1.24.

*3-(4-Methoxyphenyl)-6-(3-nitro-4-methoxyphenyl)-[1,2,4]triazolo[3,4-b][1,3,4]thiadi azole (**4o**).*

Yellow solid; yield: 73%; M.p.: 226-229 ^{o}C; ^{1}H-NMR (600 MHz, $CDCl_3$): δ 8.44 (d, *J* = 2.4 Hz, 1H), 8.30 (d, *J* = 8.9 Hz, 2H), 8.07 (dd, *J* = 8.9 Hz, *J* = 2.4 Hz, 1H), 7.27 (d, *J* = 8.9 Hz, 1H), 7.08 (d, *J* = 8.9 Hz, 2H), 4.08 (s, 3H), 3.90 (s, 3H); ^{13}C-NMR (150 MHz, $CDCl_3$): δ 163.6, 161.3, 155.7, 153.2, 146.7, 140.0, 132.4, 128.0 (2C), 124.3, 121.8, 117.9, 114.4 (2C), 114.3, 57.0, 53.3; ESI-MS: m/z = 384.1 $[M+H]^+$, 406.1 $[M+Na]^+$.

4.1.25.

*3-(4-Methoxyphenyl)-6-(3-amino-4-methoxyphenyl)-[1,2,4]triazolo[3,4-b][1,3,4]thia diazole (**4p**).*

Pale yellow solid; yield: 67%; M.p.: 169-171 ^{o}C; ^{1}H-NMR (600 MHz, DMSO-d_6): δ 8.21 (d, *J* = 8.6 Hz, 2H), 7.30 (d, *J* = 1.9 Hz, 1H), 7.17 (dd, *J* = 8.4 Hz, *J* = 1.9 Hz,

1H), 7.16 (d, *J* = 8.6 Hz, 2H), 6.97 (d, *J* = 8.4 Hz, 1H), 5.23 (s, 2H), 3.87 (s, 3H), 3.85 (s, 3H); ^{13}C-NMR (150 MHz, DMSO-d_6): δ 167.4, 161.1, 153.6, 150.4, 145.7, 139.2, 127.9 (2C), 121.9, 118.5, 116.5, 114.9 (2C), 111.0, 110.9, 56.0, 55.7; ESI-MS: m/z = 354.3 $[M+H]^+$, 376.3 $[M+Na]^+$.

4.2. Biology

4.2.1. MTT assay

The antiproliferative activities of target compounds **3a-e**, **4a-p**, ABI and SMART were determined by a standard MTT assay, as previously described [21].

4.2.2. Tubulin polymerization assay

Tubulin polymerization experiment was followed a previously reported method [22].

4.2.3. Immunofluorenscence assay

Immunofluorenscence assay studies were performed following a previously reported method [23].

4.2.4. Cell cycle analysis

Cell cycle analysis studies were performed according to procedures described previously [23-25].

4.2.5. Molecular docking

Molecular docking studies were performed following a previously documented method [24].

Acknowledgements

We gratefully acknowledge the National Natural Science Foundation of China (81673293, 81502932, 81602969), the Natural Science Foundation of Liaoning Province (201602687, 201610163L10) and State Key Laboratory of Natural Medicines and Active Substance (No. GTZK201603) for their generous financial support.

References

[1] M.A. Jordan, L. Wilson, Nat. Rev. Cancer, 4 (2004), 253–265.

[2] S. Florian, T.J. Mitchison, Methods Mol. Biol. 1413 (2016) 403–421.

[3] J.J. Field, A. Kanakkanthara, J.H. Miller, Bioorg. Med. Chem. 22 (2014) 5050–5059.

[4] Y.M. Liu, H.L. Chen, H.Y. Lee, J.P. Liou, Expert Opin. Ther. Pat. 24 (2014) 69–88.

[5] Y. Lu, J. Chen, M. Xiao, W. Li, D.D. Miller, Pharm Res. 29 (2012) 2943–2971.

[6] J. Yang , S. Yang, S. Zhou, D. Lu , L. Ji, Z. Li, S. Yu, X. Meng, Eur. J. Med. Chem. 122 (2016) 488–496.

[7] H. Mirzaei, S. Emami, Eur. J. Med. Chem. 121 (2016) 610–639.

[8] Z.Wang, H. Qi, Q. Shen, G. Lu, M. Li, K.Bao, Y. Wu, W. Zhang, Eur. J. Med. Chem. 122 (2016) 520–529.

[9] B. Sun, L. Li, Q. Hu, F. Xie, H. Zheng, H. Niu, H. Yuan, H. Lou, Eur. J. Med. Chem. 121 (2016) 484–499.

[10] N. Shobeiri, M. Rashedi, F. Mosaffa, A. Zarghi, M. Ghandadi, A. Ghasemi, R. Ghodsi, Eur. J. Med. Chem. 114 (2016) 14–23.

[11] Y. Lu, C.M. Li, Z. Wang, C.R. Ross, J. Chen, J.T. Dalton, W. Li, D.D. Miller, J. Med. Chem. 52 (2009) 1701–1711.

[12] J. Chen, Z. Wang, C.M. Li, Y. Lu, P.K. Vaddady, B. Meibohm, J.T. Dalton, D.D. Miller, W. Li, J. Med. Chem. 53 (2010) 7414–7427.

[13] L.M. Lima, E.J. Barreiro, Curr. Med. Chem. 12 (2005) 23–49.

[14] G.A. Patani, E.J. LaVoie, Chem. Rev. 96 (1996) 3147−3176.

[15] Y. Lu, J. Chen, J. Wang, C.M. Li, S. Ahn, C.M. Barrett, J.T. Dalton, W. Li, D.D. Miller, J. Med. Chem. 17 (2014) 7355−7366.

[16] U. Galli, C. Travelli, S. Aprile, E. Arrigoni, S. Torretta, G. Grosa, A. Massarotti, G. Sorba, P.L. Canonico, A.A. Genazzani, G.C. Tron, J. Med. Chem. 3 (2015) 1345−1357.

[17] P. Karegoudar, D.J. Prasad, M. Ashok, M. Mahalinga, B. Poojary, B.S. Holla, Eur. J. Med. Chem. 43 (2008) 808−815.

[18] Y.A. Ibrahim, N.A. Al-Awadi, E. John, Tetrahedron 64 (2008) 10365–10374.

[19] R. Kaur, G. Kaur, R.K. Gill, R. Soni, J. Bariwal, Eur. J. Med. Chem. 87 (2014)

89–124.

[20] R. Sita, G. Celik, P. Khloya, D. Vullo, C.T. Supuran, P.K. Sharma, Bioorg. Med. Chem. 22 (2014) 1873–1882.

[21] Q. Xu, H. Qi, M. Sun, D. Zuo, X. Jiang, Z. Wen, Z. Wang, Y. Wu, W. Zhang, PLoS ONE 10 (2015) doi:10.1371/journal.pone.0128710.

[22] Z. Wen, J. Xu, Z. Wang, H. Qi, Q. Xu, Z. Bai, Q. Zhang, K. Bao, Y. Wu, W. Zhang, Eur. J. Med. Chem. 90 (2015) 184–194.

[23] D. Zuo, D. Guo, X. Jiang, Q. Guan, H. Qi, J. Xu, Z. Li, F. Yang, W. Zhang, Y. Wu, Chemico-Biological Interactions 227 (2015) 7–17.

[24] Q. Guan, C. Han, D. Zuo, M. Zhai, Z. Li, Q. Zhang, Y. Zhai, X. Jiang, K. Bao, Y. Wu, W. Zhang, Eur. J. Med. Chem. 87 (2014) 306–315.

[25] Q. Xu, Y. Wang, J. Xu, M. Sun, H. Tian, D. Zuo, Q. Guan, K. Bao, Y. Wu, W. Zhang, ACS Med. Chem. Lett. 7 (2016) 1202–1206.

A series of antitubulin agents with a 5,5-fused-heterocycle scaffold were designed.

Compound **4f** exhibited potent antiproliferative and antitubulin activities.

Compound **4f** induced cell cycle arrest at G2/M phase.

The binding mode of **4f** was determined by docking studies.